

Implicit Variational Inference: the Parameter and the Predictor Space

Yann Pequignot* Mathieu Alain Patrick Dallaire
Alireza Yeganehparast Pascal Germain Josée Desharnais
François Laviolette

Université Laval, Québec, Canada

October 27, 2020

Having access to accurate confidence levels along with the predictions allows to determine whether making a decision is worth the risk. Under the Bayesian paradigm, the posterior distribution over parameters is used to capture model uncertainty, a valuable information that can be translated into predictive uncertainty. However, computing the posterior distribution for high capacity predictors, such as neural networks, is generally intractable, making approximate methods such as variational inference a promising alternative. While most methods perform inference in the space of parameters, we explore the benefits of carrying inference directly in the space of predictors. Relying on a family of distributions given by a deep generative neural network, we present two ways of carrying variational inference: one in *parameter space*, one in *predictor space*. Importantly, the latter requires us to choose a distribution of inputs, therefore allowing us at the same time to explicitly address the question of *out-of-distribution* uncertainty. We explore from various perspectives the implications of working in the predictor space induced by neural networks as opposed to the parameter space, focusing mainly on the quality of uncertainty estimation for data lying outside of the training distribution. We compare posterior approximations obtained with these two methods to several standard methods and present results showing that variational approximations learned in the predictor space distinguish themselves positively from those trained in the parameter space.

*Email: yann-batiste.pequignot.1@ulaval.ca

1. INTRODUCTION

As more and more industries are adopting artificial intelligence technologies, the requirements surrounding the development and deployment of AI-based systems are also evolving. In the medical sector and in aerospace for instance, several exciting applications have been developed, but will not make it to the real world until guarantees are obtained that critical mistakes can be avoided or at least safely controlled (Bhattacharyya et al., 2015; Begoli et al., 2019). Quantification of uncertainty is one important mechanism to support guarantees, therefore contributing to the safety of a system (Shafaei et al., 2018), as long as it is accurate and exhaustive. Of particular interest is the ability of a system to properly quantify uncertainty on out-of-distribution (OOD) instances, that is when predicting on instances different from the observations it learns from.

Bayesian statistical tools are a common way to tackle this challenge (MacKay, 1992; Neal, 1996). The uncertainty over a model parameters given a training set is captured within a conditional probability distribution often referred to as the *posterior distribution*. This approach is commonly extended to neural network algorithms by expressing the posterior distribution over the network parameters (*i.e.* its weights and biases). However, in most cases, the inference of this distribution is difficult to carry out due to the non-linearity and the typically large parameter space used in neural networks. Meanwhile, variational methods have gradually emerged as a time-efficient solution for obtaining an approx-

imate posterior distribution via an optimization procedure (Bishop, 2006; Wainwright and Jordan, 2008; Graves, 2011). They address the problem of intractability by finding a good approximate distribution among a given family of distributions.

Variational families for which the density is available in closed form are called *explicit families*. As these methods tend to restrict to families based on products of independent Gaussian distributions (Ranganath et al., 2014; Blundell et al., 2015; Saul and Jordan, 1996; Barber and Wiering, 1999) for computational reasons, they often lead to an underestimation of uncertainty (Turner and Sahani, 2011). Several means have been deployed to improve the capacity of explicit families such as structured or mixture families (Saul and Jordan, 1996; Bishop, 2006), but recently various methods have been proposed to implement variational inference for *implicit families*. These families trade off a density available in closed form for higher capacity and more flexibility. Among these, we have families for which the density function exists and can be efficiently computed with *invertible networks* and *normalizing flows* (Kingma et al., 2016; Dinh et al., 2016; Papamakarios et al., 2017). Finally, we have the implicit families for which the density function cannot be computed or may not even exist. The optimization in that case relies on other ideas such as Spectral Stein gradient, kernel density estimation (Li and Turner, 2017), or even adversarial density ratio estimation (Mescheder et al., 2017).

While approximating the posterior over the parameter space of a neural net is challenging, one can also wonder if the approximation should not be carried out directly in the predictor space. Indeed, as neural nets are over-parametrized prediction functions containing an exponential number of symmetries, capturing the predictive uncertainty from the point of view of the parameter space might have important limitations. Our simple approach to carrying inference directly on predictors naturally requires us to make a choice on the relative importance of possible inputs, allowing us at the same time to address explicitly the prediction of OOD uncertainty in a scalable fashion.

This paper proposes a new way to carry out variational inference using a deep generative network. Notably, we obtain state-of-the-art results using a generative network that learns to transform a normal random variable in dimension five only. Moreover, we present a way to perform inference both in the parameter space and in the predictor space by estimating the divergence of the variational

distribution from the prior using nearest neighbor (NN) estimators. We consistently use the same estimation strategy to compute empirical metrics to evaluate the learned posterior and compare it to a reasonable golden standard provided by a Markov Chain Monte Carlo (MCMC). This empirical study aims at providing a comprehensive discussion of the asset of our method for OOD uncertainty estimation as well as a general discussion on evaluation of uncertainty predictions in the case of regression.

2. OOD INFERENCE

Given a set \mathcal{D} of independent observation pairs (X, y) with input $X \in \mathbb{R}^D$ and target $y \in \mathbb{R}$, we aim at finding a model that predicts for every $X \in \mathbb{R}^D$ (of interest) a distribution over the possible targets y representing best our knowledge given our postulates and requirements.

The Bayesian regression approach proposes to tackle this task by first assuming that the data are generated according to:

$$y = f(X) + \epsilon, \quad (1)$$

where $f : \mathbb{R}^D \rightarrow \mathbb{R}$ is an unknown deterministic function and ϵ is a random variable with density $\mathcal{N}(0, \sigma_\epsilon)$. Moreover, in order to reflect that in most applications inputs do not all have the same importance, we consider that the input X in (1) is a random variable that follows either the unknown true distribution of input data or a context driven distribution that allows for an explicit focus on OOD inputs.

Postulate (1) induces the likelihood of any function $g : \mathbb{R}^D \rightarrow \mathbb{R}$ as $\mathcal{L}(g|\mathcal{D}) = \prod_{(X,y) \in \mathcal{D}} \mathcal{L}(g|X, y)$, with $\mathcal{L}(g|X, y) = p(y|X, g) = p_\epsilon(y - g(X))$, where p_ϵ is the density function of the random variable ϵ . One then further postulates or chooses a distribution P on all functions/predictors $g : \mathbb{R}^D \rightarrow \mathbb{R}$, the prior. Altogether, this allows one to define another distribution on predictors, the posterior distribution $P(g|\mathcal{D})$, whose density is given by Bayes' rule: $dP(g|\mathcal{D}) = \frac{\mathcal{L}(g|\mathcal{D})}{p(\mathcal{D})} dP(g)$, where the *marginal likelihood* (also called *evidence* and *integrated likelihood*) of the data is the usually intractable normalizing constant: $p(\mathcal{D}) = \int \mathcal{L}(g|\mathcal{D}) dP(g)$. The prediction of uncertainty about the target at input X is obtained by integration with respect to the predictive posterior as:

$$p(y|X, \mathcal{D}) = \frac{1}{p(\mathcal{D})} \int p(y|X, g) dP(g|\mathcal{D}).$$

As the evidence is in most cases intractable, we are left with the task of approximating the posterior distribution Q so as to compute the predictive uncertainty with the best accuracy. In this direction, we record the following simple and well-known fact (e.g., Murphy, 2012, §21.2) which gives a characterization of the posterior distribution in variational terms as the unique solution to an optimization problem based on the Kullback-Leibler (KL) divergence (for completeness, the proof is given in the supplementary material).

Proposition 2.1 (Variational characterization of the Bayesian posterior). *For every likelihood function $\mathcal{L}(g|\mathcal{D})$ and every prior distribution P , the Bayesian posterior distribution is the unique distribution Q that minimizes the variational objective:*

$$\mathcal{V}(Q) = - \mathbb{E}_{g \sim Q} [\ln \mathcal{L}(g|\mathcal{D})] + \text{KL}(Q, P).$$

Tractability, Predictor Representation through Neural Networks.

In practice, we do not have direct access to *all* the possible predictive functions $g : \mathbb{R}^D \rightarrow \mathbb{R}$. We have only access to some of them through a chosen representation, that is, a parametric model family. Given the success of neural networks in machine learning, they have been extensively used to model predictors in regression tasks. A network architecture comes with a specific number of parameters, say d , consisting of *weights* and *biases*. This gives rise to the parameter space \mathbb{R}^d ; henceforth, a vector $\theta \in \mathbb{R}^d$ represents an ordered list of weights and biases for the network and hence encodes a unique predictor $f_\theta : \mathbb{R}^D \rightarrow \mathbb{R}$. Abstractly, this choice of network architecture amounts to choosing a set \mathcal{F} of functions $f : \mathbb{R}^D \rightarrow \mathbb{R}$ together with a specific representation $\mathfrak{N} : \mathbb{R}^d \rightarrow \mathcal{F}$ which maps any parameter θ to a function f_θ . In the case of neural networks, this representation is such that the evaluation function $Ev : \mathbb{R}^d \times \mathbb{R}^D \rightarrow \mathbb{R}$, $(\theta, X) \mapsto f_\theta(X)$ is tractable and enjoys “nice” properties (e.g. almost everywhere infinitely differentiable).

By identifying a parameter θ with the corresponding function f_θ , it becomes possible to implement the Bayesian approach as follows. We choose a prior distribution P on parameters with tractable density function $p(\theta)$, for instance a fully factorized Gaussian distribution. We define the likelihood of a parameter θ as the likelihood of f_θ , i.e. $p(y|X, \theta) = p(y|X, f_\theta)$ and $\mathcal{L}(\theta|\mathcal{D}) = \mathcal{L}(f_\theta|\mathcal{D})$. Then we define the density function of the posterior

distribution on parameters up to a scaling factor: $p(\theta|\mathcal{D}) \propto \mathcal{L}(\theta|\mathcal{D})p(\theta)$. Since the right-hand term is tractable and (almost everywhere) differentiable, it can be used to approximate the posterior distribution using MCMC methods such as Hamiltonian Monte Carlo (HMC) methods (Betancourt, 2017). These methods yield samples $(\theta_j)_{j < N}$ of parameters which can be used to estimate the predictive uncertainty:

$$p(y|X, \mathcal{D}) = \int p(y|X, \theta)p(\theta|\mathcal{D})d\theta \approx \frac{1}{N} \sum_{j < N} p(y|X, \theta_j). \quad (2)$$

Let us note that the identification of parameters with functions has several implications. First by choosing the network architecture we restrict ourselves to a subset $\mathcal{F} = \{f_\theta \mid \theta \in \mathbb{R}^d\}$ of all functions. This is not a strong theoretical restriction, since by the Universal Approximation Theorem for neural networks we can make \mathcal{F} as close as we want from the set of all (Lebesgue measurable) functions (Cybenko, 1989). However, in practice, our methods usually only explore parameters with a small enough Euclidean norm, therefore shrinking \mathcal{F} to a smaller tractable part. Secondly, and most importantly, we have traded the mysterious infinite dimensional geometry of functions for the *ad-hoc* d -dimensional Euclidean geometry of the parameters. In particular, if f_{θ_0} and f_{θ_1} are two functions yielding very similar predictions on some data, what can we say about the Euclidean distance between θ_0 and θ_1 ?

Parametric Variational Inference. Prop. 2.1 opens an avenue for approximating the Bayesian posterior. Given the prior distribution P and the likelihood function $\mathcal{L}(\theta|\mathcal{D})$, we choose a parametric family $\mathcal{Q} = \{Q_\lambda \mid \lambda \in \mathbb{R}^l\}$ of distributions on the space \mathbb{R}^d of parameters and search for the distribution $Q \in \mathcal{Q}$ that minimizes the opposite of the *evidence lower bound* (ELBO):

$$\mathcal{V}(Q) = - \mathbb{E}_{\theta \sim Q} [\ln \mathcal{L}(\theta|\mathcal{D})] + \text{KL}(Q, P). \quad (3)$$

By substituting this variational objective for an estimator that is differentiable w.r.t. the parameters of the variational distribution Q , this minimization can be achieved using stochastic gradient descent (SGD). The need for such an estimator of the variational objective usually restricts the choice of the variational family \mathcal{Q} . The first term of Eq. (3), the expected log likelihood of the variational distribution Q given the data, rewards distributions

that concentrate on functions that predict the data accurately. It is easily estimated by a Monte Carlo (MC) estimate as long as we can sample from Q . Moreover this term does not suffer the fact that we identify f_θ with θ , since the likelihood of θ is defined as the likelihood of f_θ . The second term of Eq. (3), the KL divergence from our variational distribution Q to our prior P , rewards distributions that are close to P (in the KL sense). Moreover it rewards variational distributions whose differential entropy $H(Q)$ is large since this term can further be decomposed as $\text{KL}(Q, P) = -H(Q) - \mathbb{E}_{\theta \sim Q} \ln p(\theta)$, where $\ln p(\theta)$ denotes the log density of the prior. The latter term is harder to estimate and the computation of an MC estimate requires to have access to the log density of both the prior P and the variational distribution Q in addition to being able to sample from Q .

3. PROPOSED METHOD

We explore variational inference along two distinct but related directions. First, we consider implicit families of distributions given by generative networks such as the ones used in GANs. Second, we introduce a way of approximating the KL divergence term of the ELBO in the predictor space.

Since our generative networks learn to transform a low-dimensional fully factorized Gaussian into a higher-dimensional random variable in parameter space, the probability density function of our variational distribution is intractable both in parameter space and predictor space¹. We choose to rely on the NN estimate of the KL term both in parameter space and in predictor space.

3.1. Nearest Neighbor Estimation of KL Divergence and Entropy

We present here a coherent and simple approach to estimating KL divergences of distributions both on the parameters and the predictors based on k -nearest neighbor (kNN) distances.

The Parameter Space. Given d -dimensional independent samples $\tilde{Q} = \{q_i \mid i < N\}$ and $\tilde{P} = \{p_j \mid j < M\}$ from distributions Q and P

respectively, the kNN estimation of the KL divergence from Q to P is given by (Perez-Cruz, 2008):

$$\widehat{\text{KL}}_k(\tilde{Q}, \tilde{P}) = \ln \frac{M}{N-1} + \frac{d}{N} \sum_{i < N} \ln \frac{s_k(q_i)}{r_k(q_i)}, \quad (4)$$

where $r_k(q_i)$ and $s_k(q_i)$ denote the Euclidean distance from q_i to its k -nearest neighbor in $\tilde{Q} \setminus \{q_i\}$ and in \tilde{P} respectively. While low values of k are in principle favored to reduce bias, increasing the value of k allows us to avoid underflow imprecision when samples are very close to each other.

Importantly, the KL divergence from Q to P can be decomposed as $\text{KL}(Q, P) = -H(Q) - \mathbb{E}_Q[\ln P]$ where $H(Q)$ denotes the differential entropy of Q . The following provides an estimator of the differential entropy of Q based on samples $\tilde{Q} = \{q_i \mid i < N\}$ along the same line (Singh et al., 2003):

$$\widehat{H}_k(\tilde{Q}) = C_{d,k,N} + \frac{d}{N} \sum_{i < N} \ln r_k(q_i), \quad (5)$$

where $C_{d,k,N} = \ln(N) - \psi(k) + \ln(\pi^{\frac{d}{2}}/\Gamma(\frac{d}{2}+1))$ is a constant, $\psi(x) = \Gamma(x)'/\Gamma(x)$ is the digamma function.

The Predictor Space. Let $\Pi \in \mathbb{R}^d$ and $\Theta \in \mathbb{R}^d$ be random variables following the prior distribution P and the variational distribution Q respectively. Instead of relying on $\text{KL}(Q, P)$, we would like to consider the ‘‘KL divergence’’ from the distribution of f_Π to that of f_Θ . Since the KL estimator (4) relies solely on relative distances of the samples, it opens an avenue for formalizing this idea by substituting the Euclidean distance between parameters with a distance on functions which reflects the geometry of our predictors. What distance do we want to consider on the space of predictors? As we shall see, the Euclidean distance between two parameters θ and θ' may differ drastically from the distance between the corresponding functions f_θ and $f_{\theta'}$. For instance, because of symmetries in our network-based model, we may have $f_\theta = f_{\theta'}$ while $\|\theta - \theta'\|$ is large. It may also happen that $f_\theta(X) = f_{\theta'}(X)$ for most inputs X in the domain of interest while the parameters θ and θ' are far apart in the Euclidean space.

We therefore suggest choosing a distribution ν on the input space \mathbb{R}^D that represents the relative importance we give to all possible inputs. This choice depends on the specific task. In our experiments, we take ν to be the uniform distribution whose support is a bounded hyperrectangle $\mathcal{H} \subseteq \mathbb{R}^D$ constructed from the training data (defined in section 4). This simple input distribution serves as a model for the OOD in opposition to the *in-distribution* of

¹Note that even for Mean-Field families (MFVI) whose density function is tractable in parameter space, the density is no longer tractable in predictor space. We explored the variant of MFVI where the KL term is approximated in predictor space as FuNN-MFVI.

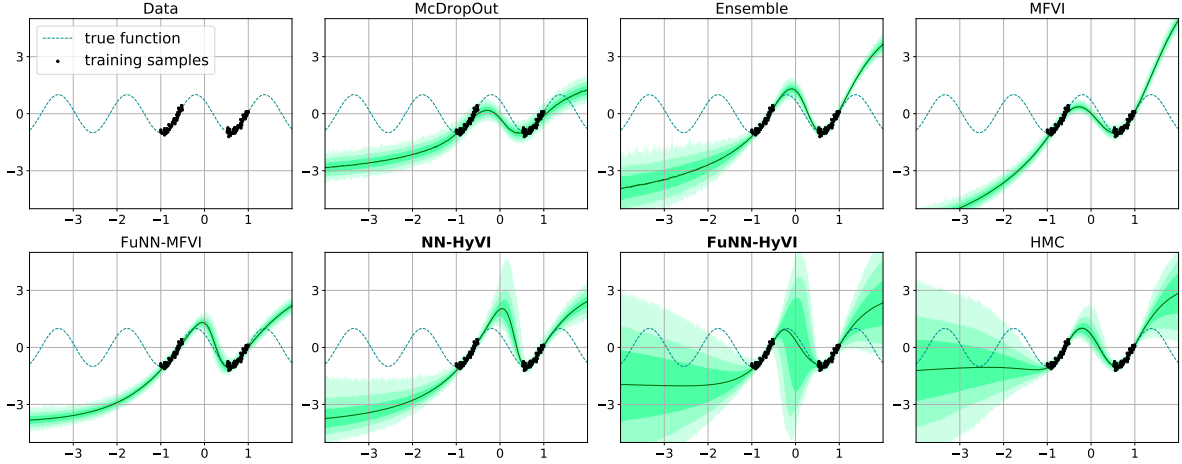


Figure 1.: Synthetic dataset: Comparison of various models for prediction of uncertainty. The solid line represents the mean of the predictions and each shade of green represents one standard deviation.

the training inputs.² But one could also use inputs from the training set and choose ν to be a mixture of the unknown distribution of input data with the chosen OOD distribution.

Choosing a distribution ν on the inputs allows us to define the *predictor space* as the Hilbert space $L_2(\nu)$ with the norm distance:

$$\|f - g\|_{L_2} = \left(\int |f(X) - g(X)|^2 d\nu(X) \right)^{\frac{1}{2}}.$$

Note that every sample $\mathcal{X} = (X_0, \dots, X_{T-1}) \sim \nu^T$ yields a MC estimate of the L_2 norm:

$$\begin{aligned} \|f - g\|_{L_2} &\approx \left(\frac{1}{T} \sum_{t < T} |f(X_t) - g(X_t)|^2 \right)^{\frac{1}{2}} \\ &= T^{-1/2} \|f^{\mathcal{X}} - g^{\mathcal{X}}\|_2, \end{aligned}$$

in terms of the Euclidean distance $\|\cdot\|_2$ between the vectors $f^{\mathcal{X}} = (f(X_0), \dots, f(X_{T-1})) \in \mathbb{R}^T$ and $g^{\mathcal{X}} = (g(X_0), \dots, g(X_{T-1})) \in \mathbb{R}^T$ obtained by evaluation. Hence each input sample \mathcal{X} yields an evaluation map $f \mapsto f^{\mathcal{X}}$ which provides a “probably approximately isometric map” from the infinite dimensional Hilbert space $L_2(\nu)$ in the Euclidean space \mathbb{R}^T up to a scaling factor of $T^{-1/2}$.

Therefore given independent samples³ $\tilde{F} = (f_i)_{i < N}$ and $\tilde{G} = (g_j)_{j < M}$ in $L_2(\nu)$ from random

²At test time on some input X , we can first check if X sits inside the hyperrectangle (reject if not) and then evaluate the uncertainty of our model on X (reject if past a given threshold) before using the prediction.

³In our experiments, the sample of functions (f_i) is obtained from a sample of parameters (θ_i) by letting f_i be the function encoded by θ_i via our network, *i.e.* $f_i = f_{\theta_i}$.

variables F and G respectively, our proposed KL divergence estimate is

$$\widehat{\text{KL}}_k^\nu(\tilde{F}, \tilde{G}) = \mathbb{E}_{\mathcal{X} \sim \nu^T} \widehat{\text{KL}}_k(\tilde{F}^{\mathcal{X}}, \tilde{G}^{\mathcal{X}}), \quad (6)$$

where the estimator from Eq. (4) is applied to the T -dimensional samples $\tilde{F}^{\mathcal{X}} = \{f_i^{\mathcal{X}}\}$ and $\tilde{G}^{\mathcal{X}} = \{g_j^{\mathcal{X}}\}$. Note that no adjustment to Eq. (4) is necessary because it only involves ratios of distances, and the scaling factor $T^{-1/2}$ cancels out.

In the same fashion, we propose to estimate the differential entropy of the random variable F from samples $\tilde{F} = \{f_i \mid i < N\}$ in $L_2(\nu)$ via:

$$\widehat{\text{H}}_k^\nu = \mathbb{E}_{\mathcal{X} \sim \nu^T} \widehat{\text{H}}_k(\tilde{F}^{\mathcal{X}}) - \frac{1}{2} \ln T, \quad (7)$$

where the constant term comes from our scaling of distances by the factor $T^{-1/2}$.

3.2. Implicit Variational Inference: Generative Networks

A generative network is simply a neural network architecture encoding a parametric family of functions $h_\lambda : \mathbb{R}^l \rightarrow \mathbb{R}^d$, where the parameter λ lists the *weights and biases* of the neural network and each h_λ transforms a Gaussian random noise $\epsilon \sim \mathcal{N}(0, \mathbf{I}_l)$ into another random variable in \mathbb{R}^d . Any parametric family $(h_\lambda)_{\lambda \in \Lambda}$ of networks therefore gives rise to the family of random variables of the form $\theta = h_\lambda(\epsilon)$. In our context, this serves as our variational family and the outputs θ of the generative network are parameters for the predictor network

f_θ . We therefore refer to the generative network as hypernet and talk about Hypernet Variational Inference (HyVI) to highlight the difference with the family of multivariate Gaussian with diagonal covariance matrix and Mean Field Variational Inference (MFVI, aka Bayes By Backprop).

In the Parameter Space: NN-HyVI. The first of our methods (Nearest Neighbor – Hypernet Variational Inference) performs inference directly in the parameter space. Given a predictor network architecture $y = f_\theta(X)$, a (possibly implicit) prior P on parameters θ and a likelihood function $\mathcal{L}(f|X, y)$, we update the parameters of the variational distribution q_λ using SGD so as to minimize on each mini-batch \mathcal{B} of training data \mathcal{D} the objective (see Alg. 1 in Suppl. Mat.)

$$\mathcal{V}(q_\lambda) = \frac{|\mathcal{B}|}{|\mathcal{D}|} \mathbb{E}_{\substack{\theta \sim q_\lambda \\ \pi \sim P}} \widehat{\text{KL}}_1(\theta, \pi) - \sum_{(X, y) \in \mathcal{B}} \mathbb{E}_{\theta \sim q_\lambda} \ln \mathcal{L}(f_\theta|X, y). \quad (8)$$

In the Predictor Space: FuNN-HyVI. Our second method (Functional Nearest Neighbor – Hypernet Variational Inference) performs inference directly in the predictor space, and uses the parameter space only as a convenient way to represent the predictor space. It also relies on a parametric model of predictors $y = f_\theta(X)$, but it further requires a distribution ν on inputs from which we can sample from. Given also a (possibly implicit) prior P on predictors and a likelihood function $\mathcal{L}(f|X, y)$, we update the parameters of a variational distribution q_λ using SGD so as to minimize on mini-batch \mathcal{B} of training data \mathcal{D} the following objective (See 2 in Suppl. Mat.):

$$\mathcal{V}(q_\lambda) = \frac{|\mathcal{B}|}{|\mathcal{D}|} \mathbb{E}_{\substack{\theta \sim q_\lambda \\ g \sim P}} \widehat{\text{KL}}_1^\nu(f_\theta, g) - \sum_{(X, y) \in \mathcal{B}} \mathbb{E}_{\theta \sim q_\lambda} \ln \mathcal{L}(f_\theta|X, y). \quad (9)$$

Since we only need to sample predictors from the prior, our method allows for the use of a prior given by a Gaussian process, for example. However in our experiments, we used a prior P on parameters and sampled predictors according to $g = f_\pi$ with $\pi \sim P$.

3.3. Related Work

Implicit Weight Uncertainty in Neural Networks. Pawlowski et al. (2017) also used an NN estimate of the KL divergence on parameters. However, it

appears that they treat each parameter independently and use an average of the KL approximations over each scalar parameter. This approach lacks a theoretical justification and the authors’ preference is only based on limited empirical evidence of its efficiency. In contrast, we address the important dependency between the parameters by using the NN estimator of the KL on parameter vectors.

FBNN. A closely related work by Sun et al. (2019) also provides a method for variational inference in predictor space. They give an interesting theoretical justification for an expression of the KL divergence from one stochastic process to another as the supremum over all finite sets of inputs of the KL divergence between corresponding marginal distributions. However, they end up using an approximation which consists of averaging over input samples the KL divergence of the corresponding marginal distributions. While this approximation is not theoretically justified in their paper, it turns out to be similar to our approximation of the KL for distributions of functions (6) which naturally arise from a novel motivation for an explicit choice of the input distribution for the MC approximation of the L_2 distance on predictors. Moreover, they use inputs from the training data in addition to OOD inputs to marginalize predictors and a Stein Spectral Gradient estimate of the gradient of the KL on marginal distributions. Two crucial differences with our FuNN-HyVI are 1) they use a variational family of multivariate Gaussian distribution with diagonal covariance matrix (as in our FuNN-MFVI which performs poorly) where we use a generative network and 2) they regularize the KL term to increase its importance in the ELBO on mini-batches where we maintain the expected gradient of the ELBO. Finally, their method also differs in that they use data-dependent Gaussian process priors where we simply use a Gaussian prior on parameters.

4. EMPIRICAL STUDY

Our experiments aimed primarily at evaluating the quality of the uncertainty predicted with our methods. In accordance with the literature we computed the root-mean-square error (RMSE) and log Posterior Predictive (LPP) on held out test data, but we also considered other metrics to evaluate the uncertainty of the model as a whole and as well as its ability to detect OOD inputs.

| | HMC | NN-HyVI | FuNN-HyVI |
|------------------------|------|------------------|-----------------|
| Parameter Space | | | |
| boston | 971 | 1564 ± 11 | 420 ± 25 |
| concrete | 637 | 1088 ± 6 | 332 ± 18 |
| energy | 627 | 1086 ± 9 | 223 ± 34 |
| wine | 614 | 1412 ± 28 | -1507 ± 32 |
| yacht | 503 | 763 ± 6 | 149 ± 35 |
| Predictor Space | | | |
| boston | -51 | -413 ± 5 | 317 ± 15 |
| concrete | -106 | -435 ± 2 | 273 ± 2 |
| energy | -225 | -243 ± 8 | 146 ± 11 |
| wine | -28 | -250 ± 9 | 278 ± 9 |
| yacht | -246 | -663 ± 10 | 91 ± 4 |

Table 1.: Entropy of posterior distributions

Entropy of Posterior Distributions We computed the differential entropy of the posterior distributions based on $1K$ samples both in parameter space using (5) and in predictor space using an MC estimate of (7) based on 100 samples from ν^{200} .

Epistemic Uncertainty We measured the epistemic uncertainty predicted on training inputs, test inputs and $1K$ samples from ν . For each input X , we sample $1K$ scalar predictions using our model (ignoring the aleatoric uncertainty when available) and use (5) to estimate the entropy of this 1D distribution.

4.1. Experimental Setup

We experimented on a synthetic dataset and 9 UCI regression datasets (5 small, 4 large).

Synthetic Data. We generated a training set consisting of 120 pairs (X, y) with inputs X sampled uniformly from $[-1., -0.5] \cup [0.5, 1.]$ using the function $y = \cos(4(X+0.2)) + \epsilon$, with $\epsilon \sim \mathcal{N}(0., 0.1)$. The OOD distribution ν is uniform on $[-4., 2.]$.

Real World Datasets. These datasets were downloaded from the UCI machine learning repository (Dua and Graff, 2017) and include the small datasets, Boston Housing ($D = 13, N = 506$), Concrete Compressive Strength (8,1030), Energy (8, 768), Wine Quality Red (11, 1599), Yacht Hydrodynamics (6, 308) and the large datasets, Power Plant Combined Cycle (4, 9568), kin8nm (8, 8192), Condition Based Maintenance of Naval Propulsion

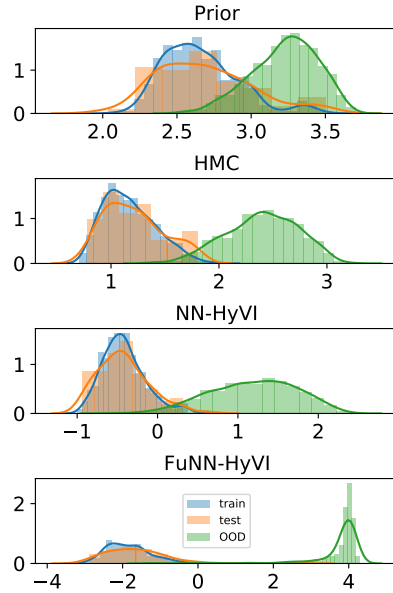


Figure 2.: Distributions of the epistemic uncertainty on train, test and OOD inputs on the Concrete UCI dataset. Similar results are in supplementary material.

Plants Compressor (16, 11034) and Protein Data (9, 45730). We have split each dataset in training (90%) and test (10%). For the input distribution ν , we used a uniform distribution on a rectangle based on the input train data which serves as a proxy for the OOD. More specifically, each feature was sampled uniformly from $[x_{\min}, x_{\max}]$ where x_{\min} and x_{\max} are respectively the minimum and maximum value taken by this feature in the dataset.

Predictor Network. For the synthetic dataset, we used a single layer network with 50 hidden units and Tanh activations. For the UCI datasets, we used a single layer with ReLU activations and 50 hidden units for the small ones, 100 for the large ones.

Prior In all our experiments, we used the same Gaussian prior on the parameters of the predictor network with zero mean and covariance matrix $0.5\mathbf{I}$.

4.2. Experiments

Toy Experiment We compared various methods to predict uncertainty on our synthetic dataset, using when possible $\sigma_l = 0.1$ (the noise chosen for the data generation) for the likelihood.

| RMSE | HMC | NN-HyVI | FuNN-HyVI |
|----------|--------------|--------------------------|--------------------------|
| boston | 2.636 | 2.683 \pm 0.02 | 3.247 \pm 0.22 |
| concrete | 7.459 | 6.683 \pm 0.17 | 5.481 \pm 0.31 |
| energy | 2.619 | 0.783 \pm 0.03 | 0.491 \pm 0.00 |
| wine | 0.583 | 0.682 \pm 0.02 | 0.686 \pm 0.02 |
| yacht | 3.853 | 1.389 \pm 0.07 | 1.168 \pm 0.10 |
| LPP | HMC | NN-HyVI | FuNN-HyVI |
| boston | -4.113 | -4.075 \pm 1e-4 | -4.085 \pm 9e-4 |
| concrete | -5.272 | -5.252 \pm 3e-4 | -5.252 \pm 3e-4 |
| energy | -3.607 | -3.565 \pm 2e-4 | -3.562 \pm 1e-5 |
| wine | -0.9 | -1.356 \pm 0.08 | -1.455 \pm 0.09 |
| yacht | -4.07 | -4.003 \pm 2e-4 | -4.001 \pm 3e-4 |

Table 2.: RMSE and LPP for Exp. 1.

Experiment 1 For each small UCI dataset, we chose a specific random train/test split and a fixed noise (see Section C in Suppl. Mat.). Then we used HMC to estimate the posterior distribution and we ran three times with random initialization both NN-HyVI and FuNN-HyVI.

Experiment 2 We executed the various methods on 10 random splits (5 for the large UCI datasets) to account for variability in the datasets, jointly learning the likelihood noise as a parameter of the ELBO when possible.

4.3. Implementation details

Generative Network Training (HyVI). For both NN-HyVI and FuNN-HyVI, we used a generative network with ReLU activations transforming 5-dimensional Gaussian samples $\mathcal{N}(0, \mathbf{I}_5)$ via a first layer with 20 hidden units and a second layer with 40 hidden units (the number of output units equals the number of parameters of the predictor network). This hypernet was trained using Adam optimizer to explore a learning rate in $[0.005, 0.0001]$ decreasing by a ratio of 0.7 when no progress is made in the variational objective after a patience of 30 epochs. We used mini-batches of size 50 except on the large UCI datasets, where we used a size of 500.

NN-HyVI. We used 100 samples of the variational distribution for evaluating the expected log likelihood. For estimating the KL with $\widehat{\text{KL}}_1$, we used 500 samples from each of the variational distribution and the prior.

FuNN-HyVI. We similarly sampled a 100 times from the variational distribution for evaluating the expected log likelihood. For approximating the KL in predictor space using $\widehat{\text{KL}}_1^\nu$, we sample 500 times from each of variational distribution and the prior and evaluate each of them at a single sample from ν^T . On the synthetic examples, we used $T = 50$, whereas on the UCI datasets we used $T = 200$.

Other methods We compare our methods to HMC (Betancourt, 2017), MC dropout (Gal and Ghahramani, 2016), Ensemble (Lakshminarayanan et al., 2017), MFVI (Blundell et al., 2015) (details in Suppl. Mat.) and the following variant of MFVI.

FuNN-MFVI. The parameters of the Gaussian posterior (jointly with the likelihood noise σ_l in Exp. 2) were trained using the ELBO as objective. We used the same approximation of the ELBO as in FuNN-HyVI (9) with same mini-batch size, optimizer and learning rate scheme as for NN-HyVI and FuNN-HyVI.

4.4. Results

In this section, we raise empirical evidence that carrying out the inference in predictor space, such as done by FuNN-HyVI, indeed yields a higher epistemic uncertainty of the whole model, a property which translates into robustness for OOD detection. This suggests that variational inference in predictor space could lead to higher quality uncertainty than the computationally demanding golden standard provided by MCMC methods, such as HMC, which are restricted to the parameter space of the network.

Synthetic Data. We plotted the uncertainty predicted by the various methods on our synthetic dataset in Fig. 1. We find that MC dropout, MFVI, FuNN-MFVI all fail to estimate the uncertainty. Ensemble struggles to predict higher uncertainty on OOD, especially in the region between the two patches. NN-HyVI predicts higher uncertainty on OOD but still provide an underestimation on the boundaries of the interval ($X = -4.$ and $X = 2.$) in comparison with HMC and FuNN-HyVI. Finally, we find that FuNN-HyVI (run time: 12 seconds) provides an uncertainty prediction that is quite close to HMC (run time: 15 hours) while being even less confident on OOD, especially in the region between the two patches.

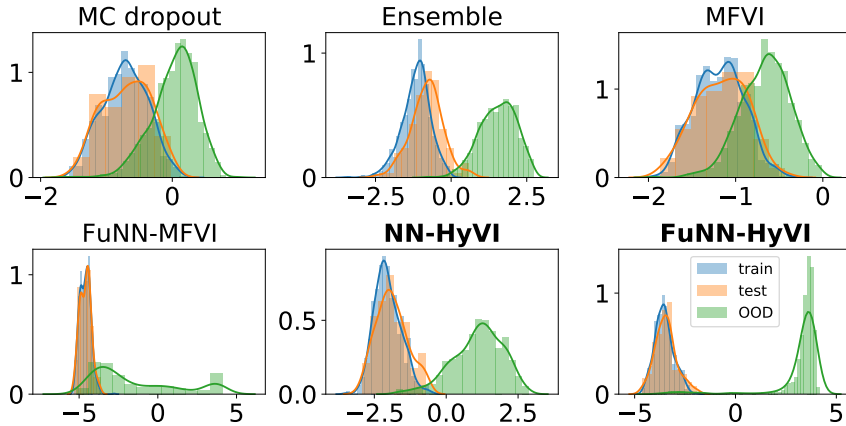


Figure 3.: Distributions of epistemic uncertainty on Concrete UCI dataset. Similar results in Suppl. Mat.

| RMSE | MC dropout | Ensemble | MFVI | FuNN-MFVI | NN-HyVI | FuNN-HyVI | FBNN† |
|------------|-------------------|-------------------------------------|-------------------|-------------------|-------------------------------------|-------------------------------------|-------------------------------------|
| kin8nm | $0.0788 \pm 1e-3$ | $0.0723 \pm 1e-3$ | $0.0754 \pm 2e-3$ | $0.0732 \pm 1e-3$ | $0.0705 \pm 1e-3$ | $0.0699 \pm 2e-3$ | NA |
| navalC | $0.0008 \pm 1e-5$ | $0.0004 \pm 3e-5$ | $0.0004 \pm 6e-5$ | $0.0007 \pm 1e-4$ | $0.0002 \pm 1e-5$ | $0.0002 \pm 4e-6$ | 0.0001 ± 0.00 |
| powerplant | 4.0071 ± 0.06 | 3.9765 ± 0.06 | 4.0057 ± 0.05 | 3.9464 ± 0.06 | 3.9122 ± 0.05 | 3.9003 ± 0.07 | NA |
| protein | 4.4312 ± 0.03 | 4.0978 ± 0.03 | 4.3275 ± 0.04 | 4.179 ± 0.02 | 4.1531 ± 0.02 | 4.1481 ± 0.03 | 4.326 ± 0.01 |

| LPP | MC dropout | Ensemble | MFVI | FuNN-MFVI | NN-HyVI | FuNN-HyVI | FBNN† |
|------------|-------------------|--------------------|-------------------|-------------------|------------------------------------|-------------------------------------|------------------|
| kin8nm | 1.107 ± 0.01 | -2.014 ± 0.27 | 1.162 ± 0.02 | 1.182 ± 0.01 | 1.221 ± 0.02 | 1.211 ± 0.03 | NA |
| navalC | 5.085 ± 0.01 | 5.408 ± 0.25 | 6.449 ± 0.17 | 5.904 ± 0.16 | 6.91 ± 0.05 | 7.192 ± 0.02 | 7.13 ± 0.01 |
| powerplant | -2.811 ± 0.01 | -58.377 ± 5.73 | -2.807 ± 0.01 | -2.792 ± 0.02 | -2.784 ± 0.01 | -2.782 ± 0.02 | NA |
| protein | -2.91 ± 0.01 | -14.811 ± 1.03 | -2.884 ± 0.01 | -2.849 ± 0.01 | -2.843 ± 0.0 | -2.842 ± 0.01 | -2.892 ± 0.0 |

Table 3.: RMSE and LPP for Exp. 2. Similar results on small UCI datasets are in Suppl. Mat. †: Reported from Sun et al. (2019)

Epistemic Uncertainty of Posterior Distributions.

We report in Table 1 the differential entropy with mean and standard error for Exp. 1. When considered as distribution on parameters, on all datasets NN-HyVI achieves a larger entropy than HMC, while FuNN-HyVI always has the smallest entropy. On the contrary, in predictor space, FuNN-HyVI achieves the largest entropy followed by HMC and finally by NN-HyVI. This can be explained by the fact the entropy in parameter space is part of the objective of NN-HyVI, while the entropy in predictive space is part of the objective of FuNN-HyVI. This also provides evidence that there is no direct relation between the entropy in parameter space and the entropy in predictor space. We consider that this also supports our claim that the inference in the parameter space is made (artificially) hard by the *ad hoc* representation of predictors induced by the choice of the network architecture.

Moreover, we suggest that the entropy of the posterior in predictor space is a good measure of the epistemic uncertainty of the overall variational model with respect to the chosen OOD distribution. Given that HMC and NN-HyVI carry out inference in parameter space, we note that HMC performs better than NN-HyVI since it achieves a larger entropy in predictor space with a smaller entropy in parameter space. However, FuNN-HyVI has the best performance in this respect.

OOD Detection. Distributions of epistemic uncertainty predicted on train, test and OOD inputs are displayed in Fig. 2 and 3, (resp. EXP. 1 and 2). Note that our prior turns out to be more certain on data than it is on OOD inputs. We observe that MC dropout, MFVI and FuNN-MFVI all fail to distinguish OOD data from train/test data. While HMC, NN-HyVI and Ensemble all make a distinc-

tion, FuNN-HyVI is by far the only method to clearly separate the OOD inputs from train/test data based on epistemic uncertainty. This crucial property which can be leveraged to perform OOD detection singles out FuNN-HyVI.

In particular, this empirical result together with that of Table 1 suggests that carrying out inference in predictor space using a hypernet opens a promising avenue for efficient prediction of uncertainty beyond the HMC.

Metrics on Test Data. We report mean and standard error for RMSE and LPP in Tab. 2 (Exp.1) and in Tab. 3 (Exp.2). Results for Exp 1. show that overall NN-HyVI and FuNN-HyVI perform similarly or a little better than HMC in terms of LPP and RMSE on test. This contrasts with our results on the entropy of the corresponding posterior distribution and the histograms of epistemic uncertainty, therefore casting serious doubts about the ability of RMSE and LPP to assess the quality of uncertainty in OOD situations. For Exp. 2, our results showed that our algorithms are competitive with the state-of-the-art on both RMSE and LPP, with a slight advantage for FuNN-HyVI.

5. CONCLUSION

Every method for predicting uncertainty with neural networks rely on a specific way to collect a diversity of predictors. MCMC methods use a random walk, Ensemble methods use the randomness inherent to initialization and training, variational inference methods rely on maximizing the differential entropy. While most methods seek diversity in parameter space, we found empirical evidence that a diversity of parameters—as measured by entropy—does not mean a diversity of predictors. We presented a simple approach to estimating the Kullback-Leibler divergence and the differential entropy for distributions of predictors based on the choice of an OOD distribution. We used this idea to optimize a deep generative network serving as implicit variational distribution. Among the methods we considered, we find that FuNN-HyVI, which combines the hypernet variational family and a variational objective in predictor space, is the only one to systematically produce a posterior whose epistemic uncertainty distinguishes clearly between the data and the OOD. This empirical evidence suggests that the diversity of predictors learned by FuNN-HyVI by maximizing entropy directly in

predictor space provides a robust predictive epistemic uncertainty for OOD detection, challenging the golden standard of MCMC posterior estimation which is restricted to the parameter space.

Acknowledgments

This work was partially supported by the Natural Sciences and Engineering Research Council of Canada (NSERC) (IRCPJ 529529-17) and a Canadian insurance company, the NSERC Discovery Grant 114090, and the Canada CIFAR AI Chair Program. The authors also acknowledge the support of the DEEL project and thank Thomas Reid at Bombardier Inc. for his collaboration in an early stage of this research.

References

- Barber, D. and Wierginck, W. (1999). Tractable variational structures for approximating graphical models. In *NIPS*, pages 183–189.
- Begoli, E., Bhattacharya, T., and Kusnezov, D. (2019). The need for uncertainty quantification in machine-assisted medical decision making. *Nature*.
- Betancourt, M. (2017). A conceptual introduction to hamiltonian monte carlo. *arXiv: Methodology*.
- Bhattacharyya, S., Cofer, D., Musliner, D., Mueller, J., and Engstrom, E. (2015). Certification considerations for adaptive systems. In *2015 International Conference on Unmanned Aircraft Systems (ICUAS)*, pages 270–279. IEEE.
- Bishop, C. M. (2006). *Pattern Recognition and Machine Learning (Information Science and Statistics)*. Springer-Verlag, Berlin, Heidelberg.
- Blundell, C., Cornebise, J., Kavukcuoglu, K., and Wierstra, D. (2015). Weight uncertainty in neural network. In *ICML*, volume 37, pages 1613–1622.
- Carroll, C. (2019). Just a little MCMC. <https://github.com/ColCarroll/minimc>.
- Cybenko, G. (1989). Approximation by superpositions of a sigmoidal function. *Mathematics of Control, Signals and Systems*, 2:303–314.
- Dinh, L., Sohl-Dickstein, J., and Bengio, S. (2016). Density estimation using real nvp. *arXiv preprint arXiv:1605.08803*.

- Dua, D. and Graff, C. (2017). UCI machine learning repository.
- Gal, Y. and Ghahramani, Z. (2016). Dropout as a bayesian approximation: Representing model uncertainty in deep learning. In *international conference on machine learning*, pages 1050–1059.
- Graves, A. (2011). Practical variational inference for neural networks. In *NIPS*, pages 2348–2356.
- Kingma, D. P., Salimans, T., Jozefowicz, R., Chen, X., Sutskever, I., and Welling, M. (2016). Improved variational inference with inverse autoregressive flow. In *NIPS*, page 4743–4751.
- Lakshminarayanan, B., Pritzel, A., and Blundell, C. (2017). Simple and scalable predictive uncertainty estimation using deep ensembles. In *Advances in neural information processing systems*, pages 6402–6413.
- Li, Y. and Turner, R. E. (2017). Gradient estimators for implicit models. *arXiv preprint arXiv:1705.07107*.
- MacKay, D. J. C. (1992). A practical bayesian framework for backpropagation networks. *Neural Comput.*, 4(3):448–472.
- Mescheder, L., Nowozin, S., and Geiger, A. (2017). Adversarial variational bayes: Unifying variational autoencoders and generative adversarial networks. In *Proceedings of the 34th International Conference on Machine Learning-Volume 70*, pages 2391–2400. JMLR. org.
- Murphy, K. P. (2012). *Machine Learning: A Probabilistic Perspective*. The MIT Press.
- Neal, R. M. (1996). *Bayesian Learning for Neural Networks*. Springer-Verlag, Berlin, Heidelberg.
- Papamakarios, G., Pavlakou, T., and Murray, I. (2017). Masked autoregressive flow for density estimation. In *Advances in Neural Information Processing Systems*, pages 2338–2347.
- Pawlowski, N., Brock, A., Lee, M. C., Rajchl, M., and Glocker, B. (2017). Implicit weight uncertainty in neural networks. *arXiv preprint arXiv:1711.01297*.
- Perez-Cruz, F. (2008). Kullback-leibler divergence estimation of continuous distributions. In *2008 IEEE International Symposium on Information Theory*, pages 1666–1670.
- Ranganath, R., Gerrish, S., and Blei, D. (2014). Black box variational inference. In *AISTATS*, pages 814–822.
- Saul, L. K. and Jordan, M. I. (1996). Exploiting tractable substructures in intractable networks. In *NIPS*, pages 486–492.
- Shafaei, S., Kugele, S., Osman, M. H., and Knoll, A. (2018). Uncertainty in machine learning: A safety perspective on autonomous driving. In *International Conference on Computer Safety, Reliability, and Security*, pages 458–464. Springer.
- Singh, H., Misra, N., Hnizdo, V., Fedorowicz, A., and Demchuk, E. (2003). Nearest neighbor estimates of entropy. *American Journal of Mathematical and Management Sciences*, 23(3-4):301–321.
- Sun, S., Zhang, G., Shi, J., and Grosse, R. B. (2019). Functional variational bayesian neural networks. In *7th International Conference on Learning Representations, ICLR 2019, New Orleans, LA, USA, May 6-9, 2019*. OpenReview.net.
- Turner, R. E. and Sahani, M. (2011). Two problems with variational expectation maximisation for time-series models. In Barber, D., Cemgil, T., and Chiappa, S., editors, *Bayesian Time series models*, chapter 5, pages 109–130. Cambridge University Press.
- Vehtari, A., Gelman, A., Simpson, D., Carpenter, B., and Burkner, P.-C. (2019). Rank-normalization, folding, and localization: An improved \hat{R} for assessing convergence of MCMC. *arXiv: Computation*.
- Wainwright, M. J. and Jordan, M. I. (2008). Graphical models, exponential families, and variational inference. *Found. Trends Mach. Learn.*, 1(1-2):1–305.

Supplementary Material

A. Variational characterization of the Bayesian posterior distribution

For every likelihood function $\mathcal{L}(g|\mathcal{D})$ and every prior distribution P , the Bayesian posterior distribution $P(g|\mathcal{D})$ is the unique distribution Q that minimizes the variational objective

$$\mathcal{V}(Q) = -\mathbb{E}_{g \sim Q} [\ln \mathcal{L}(g|\mathcal{D})] + \text{KL}(Q, P). \quad (10)$$

Proof. Recall that for every distribution Q and Q' we have $\text{KL}(Q, Q') \geq 0$ with equality iff $Q=Q'$. Note that for every distribution Q , we have

$$0 \leq \text{KL}(Q, P(g|\mathcal{D})) = \int \ln \left(\frac{dQ}{dP(g|\mathcal{D})} \right) dQ(g) = \text{KL}(Q, P) - \int \ln \mathcal{L}(g|\mathcal{D}) dQ(g) + \ln p(\mathcal{D}),$$

with equality iff $Q = P(g|\mathcal{D})$. Hence for every distribution Q we have

$$-\ln p(\mathcal{D}) \leq \text{KL}(Q, P) - \int \ln \mathcal{L}(g|\mathcal{D}) dQ(g),$$

with equality iff $Q = P(g|\mathcal{D})$. Since $p(\mathcal{D})$ does not depend on Q , it follows that the Bayesian posterior $P(g|\mathcal{D})$ is the unique distribution that minimizes (10), as desired. \square

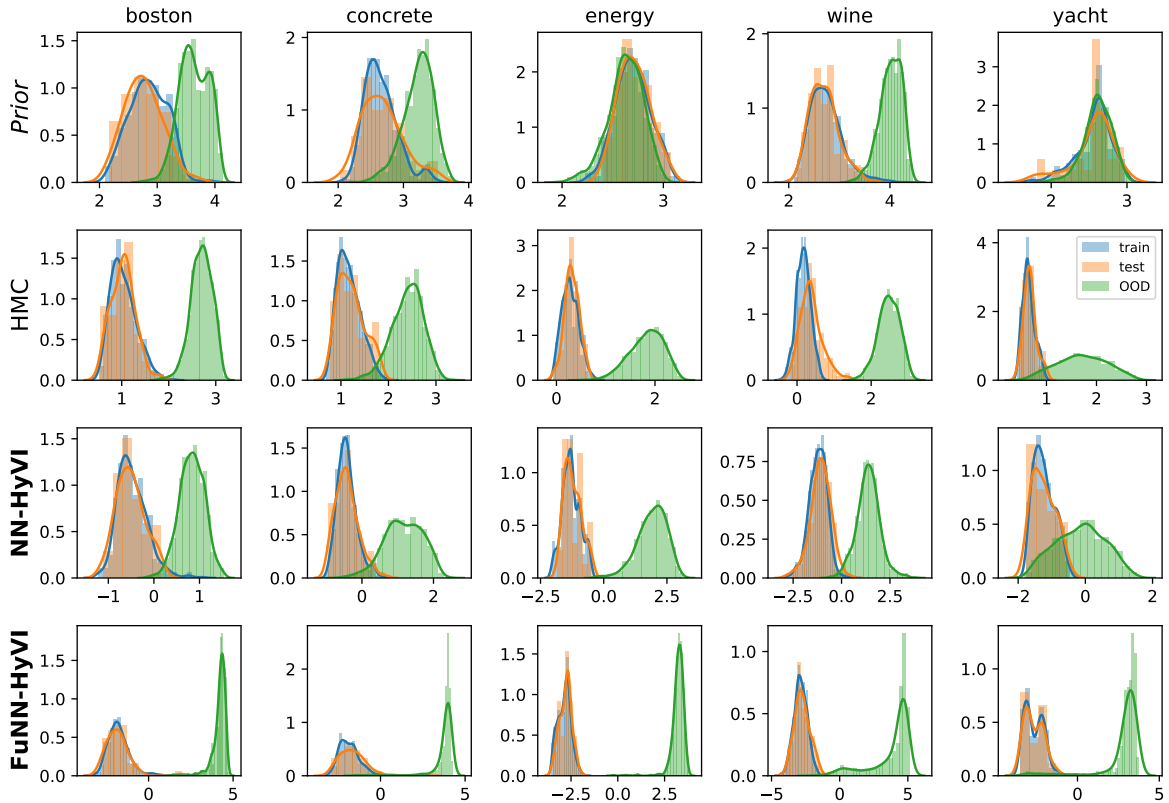


Figure 4.: Distribution of epistemic uncertainty on train, test and OOD inputs for Exp. 1.

B. Pseudo code

We include pseudo-code for NN-HyVI and FuNN-HyVI as Algorithm 1 and 2.

Algorithm 1. NN-HyVI

Require: data \mathcal{D} , likelihood $\mathcal{L}(f|X, y)$, prior distribution P

Require: parametric predictive model $y = f_\theta(X)$

Require: generative network $\theta = h_\lambda(\epsilon)$ with noise $\epsilon \sim \mathcal{N}$ and initial parameters λ

```

1: while  $\lambda$  has not converged do
2:    $\epsilon_i \sim \mathcal{N}, i < N$  ▷ Sample noise
3:    $\theta_i = h_\lambda(\epsilon_i)$  ▷ Compute parameters
4:    $\mathcal{B} \subseteq \mathcal{D}$  ▷ Get training mini-batch
5:    $\text{LL} = \frac{1}{N} \sum_{i < N} \sum_{(X,y) \in \mathcal{B}} \ln \mathcal{L}(\theta_i|X, y)$  ▷ Expected log-likelihood
6:    $\pi_j \sim P, j < N$  ▷ Sample from prior
7:    $\text{KL} = \widehat{\text{KL}}_1((\theta_i)_{i < N}, (\pi_j)_{j < N})$  ▷ KL approximation
8:    $\mathcal{V}(\lambda) = \frac{|\mathcal{B}|}{|\mathcal{D}|} \text{KL} - \text{LL}$  ▷ Compute ELBO for mini-batch
9:    $\lambda \leftarrow \text{Optimizer}(\lambda, \nabla_\lambda \mathcal{V})$ 
10: end while

```

Algorithm 2. FuNN-HyVI

Require: data \mathcal{D} , likelihood $p(y|X, f)$, prior distribution P

Require: parametric predictive model $y = f_\theta(X)$

Require: generative network $\theta = h_\lambda(\epsilon)$ with noise $\epsilon \sim \mathcal{N}$ and initial parameters λ

Require: input distribution ν

```

1: while  $\lambda$  has not converged do
2:    $\epsilon_i \sim \mathcal{N}, i < N$  ▷ Sample noise
3:    $\theta_i = h_\lambda(\epsilon_i), i < N$  ▷ Compute parameters
4:    $\mathcal{B} \subseteq \mathcal{D}$  ▷ Get training mini-batch
5:    $\text{LL} = \frac{1}{N} \sum_{i < N} \sum_{(X,y) \in \mathcal{B}} \ln \mathcal{L}(\theta_i|X, y)$  ▷ Expected log-likelihood
6:    $g_j \sim P, j < N$  ▷ Sample from prior
7:    $\mathcal{X} = (X_t)_{t < T} \sim \nu^T$  ▷ Sample inputs
8:    $f_{\theta_i}^{\mathcal{X}} = (f_{\theta_i}(X_t))_{t < T}, g_j^{\mathcal{X}} = (g_j(X_t))_{t < T}, j < N$  ▷ Evaluate predictors at these inputs
9:    $\text{KL} = \widehat{\text{KL}}_1((f_{\theta_i}^{\mathcal{X}})_{i < N}, (g_j^{\mathcal{X}})_{j < N})$  ▷ KL approximation
10:   $\mathcal{V}(\lambda) = \frac{|\mathcal{B}|}{|\mathcal{D}|} \text{KL} - \text{LL}$  ▷ Compute ELBO for mini-batch
11:   $\lambda \leftarrow \text{Optimizer}(\lambda, \nabla_\lambda \mathcal{V})$  ▷ Update parameters
12: end while

```

C. Details and more results for Experiment 1

The values for the fixed noise we used in the likelihood for Exp. 1 (after normalization) are inspired by the grid search chosen by (Gal and Ghahramani, 2016) for MC dropout: boston ($\sigma_l = 2.5$), concrete (4.5), energy (1.4), wine (0.5), yacht (1.4).

For Experiment 1, we also compared each of the 3 runs of NN-HyVI and FuNN-HyVI to the posterior reached by HMC in terms of KL divergence. Relying on 1K samples from each model, we used the nearest neighbor estimator $\widehat{\text{KL}}_1$ in parameter space and our corresponding estimator $\widehat{\text{KL}}_1^\nu$ in predictor space based on 100 samples from ν^{200} . We reported each time the average value of the three runs and the standard error in Table 4. We also computed similarly the KL divergence for each ordered pair of models to evaluate the variability of each method (column KL(-,-)).

The distributions of epistemic uncertainty for Exp. 1 and for the prior are presented in Fig. 4.

| | NN-HyVI | | | FuNN-HyVI | | |
|-----------------|--------------|---------------|---------------|----------------|---------------|----------------|
| | KL(-,HMC) | KL(HMC,-) | KL(-,-) | KL(-,HMC) | KL(HMC,-) | KL(-,-) |
| Parameter space | | | | | | |
| boston | 144.7 ± 5.60 | 487.2 ± 3.20 | 272.6 ± 1.00 | 1670.6 ± 24.60 | 960.3 ± 53.80 | 1586.0 ± 10.90 |
| concrete | 75.0 ± 2.70 | 347.7 ± 26.20 | 132.7 ± 4.20 | 1222.6 ± 5.30 | 841.7 ± 11.10 | 1197.9 ± 2.10 |
| energy | 91.2 ± 5.20 | 396.8 ± 19.50 | 173.5 ± 7.10 | 1146.3 ± 40.80 | 665.1 ± 27.80 | 1223.0 ± 24.50 |
| wine | 222.9 ± 5.90 | 734.8 ± 30.50 | 312.1 ± 19.10 | 2791.3 ± 33.90 | 650.4 ± 10.50 | 2952.5 ± 7.90 |
| yacht | 98.6 ± 3.10 | 238.0 ± 1.10 | 144.0 ± 4.80 | 997.9 ± 30.10 | 580.8 ± 5.40 | 1013.6 ± 40.10 |
| Predictor space | | | | | | |
| boston | 29.4 ± 1.70 | 265.0 ± 6.30 | 30.2 ± 1.50 | 303.2 ± 12.80 | -20.1 ± 4.90 | 20.6 ± 10.20 |
| concrete | 5.8 ± 0.80 | 260.2 ± 1.60 | 26.0 ± 4.60 | 301.0 ± 3.90 | -32.0 ± 0.60 | 5.2 ± 0.70 |
| energy | 75.2 ± 21.90 | 128.2 ± 12.90 | 103.5 ± 30.30 | 298.3 ± 9.70 | -22.5 ± 2.20 | 19.8 ± 3.30 |
| wine | 126.3 ± 5.60 | 377.9 ± 15.60 | 390.3 ± 8.90 | 244.5 ± 4.80 | 85.5 ± 5.20 | 47.4 ± 7.50 |
| yacht | 26.7 ± 4.10 | 318.5 ± 7.00 | 47.5 ± 8.90 | 277.8 ± 3.10 | -4.7 ± 0.80 | 16.0 ± 1.30 |

Table 4.: KL divergence with HMC and among models in parameter space and predictor space for Exp. 1.

D. More results for Experiment 2

We report mean and standard error for RMSE and LPP for Experiment 2 on all UCI datasets in Table 5 and plots of the distributions of epistemic uncertainty on train, test and OOD data in Fig. 5.

| RMSE | MC dropout | Ensemble | MFVI | FuNN-MFVI | NN-HyVI | FuNN-HyVI | FBNN† |
|------------|----------------------|----------------------|---------------|---------------------|----------------------|----------------------|----------------------|
| boston | 3.4 ± 0.33 | 3.468 ± 0.27 | 3.696 ± 0.39 | 3.984 ± 0.25 | 3.729 ± 0.47 | 4.33 ± 0.38 | 2.378 ± 0.03 |
| concrete | 4.869 ± 0.13 | 4.18 ± 0.24 | 5.425 ± 0.14 | 4.605 ± 0.18 | 4.48 ± 0.16 | 4.779 ± 0.21 | 4.935 ± 0.06 |
| energy | 1.106 ± 0.08 | 0.413 ± 0.02 | 0.46 ± 0.02 | 0.402 ± 0.02 | 0.452 ± 0.04 | 0.437 ± 0.03 | 0.412 ± 0.01 |
| wine | 0.635 ± 0.01 | 0.647 ± 0.01 | 0.645 ± 0.01 | 0.738 ± 0.01 | 0.721 ± 0.02 | 0.82 ± 0.03 | 0.673 ± 0.00 |
| yacht | 0.809 ± 0.09 | 0.632 ± 0.04 | 0.791 ± 0.08 | 0.699 ± 0.09 | 0.652 ± 0.08 | 0.863 ± 0.09 | 0.607 ± 0.02 |
| kin8nm | 0.0788 ± 1e-3 | 0.0723 ± 1e-3 | 0.0754 ± 2e-3 | 0.0732 ± 1e-3 | 0.0705 ± 1e-3 | 0.0699 ± 2e-3 | NA |
| navalC | 0.0008 ± 1e-5 | 0.0004 ± 3e-5 | 0.0004 ± 6e-5 | 0.0007 ± 1e-4 | 0.0002 ± 1e-5 | 0.0002 ± 4e-6 | 0.0001 ± 0.00 |
| powerplant | 4.0071 ± 0.06 | 3.9765 ± 0.06 | 4.0057 ± 0.05 | 3.9464 ± 0.06 | 3.9122 ± 0.05 | 3.9003 ± 0.07 | NA |
| protein | 4.4312 ± 0.03 | 4.0978 ± 0.03 | 4.3275 ± 0.04 | 4.179 ± 0.02 | 4.1531 ± 0.02 | 4.1481 ± 0.03 | 4.326 ± 0.01 |
| LPP | MC dropout | Ensemble | MFVI | FuNN-MFVI | NN-HyVI | FuNN-HyVI | FBNN† |
| boston | -2.82 ± 0.21 | -8.049 ± 1.33 | -2.969 ± 0.26 | -12.612 ± 2.17 | -4.342 ± 0.97 | -10.631 ± 1.95 | -2.301 ± 0.01 |
| concrete | -3.001 ± 0.02 | -6.066 ± 0.53 | -3.121 ± 0.03 | -3.518 ± 0.15 | -3.165 ± 0.11 | -3.463 ± 0.17 | -3.096 ± 0.01 |
| energy | -1.814 ± 0.03 | -2.694 ± 0.34 | -0.666 ± 0.05 | -0.891 ± 0.18 | -0.611 ± 0.09 | -0.811 ± 0.15 | -0.684 ± 0.01 |
| wine | -0.977 ± 0.03 | -3.428 ± 0.28 | -0.981 ± 0.02 | -1.813 ± 0.08 | -1.342 ± 0.06 | -2.167 ± 0.15 | -1.04 ± 0.00 |
| yacht | -1.64 ± 0.01 | -8.466 ± 2.05 | -3.348 ± 1.14 | -10.645 ± 5.06 | -0.976 ± 0.18 | -2.056 ± 0.36 | -1.033 ± 0.01 |
| kin8nm | 1.107 ± 0.01 | -2.014 ± 0.27 | 1.162 ± 0.02 | 1.182 ± 0.01 | 1.221 ± 0.02 | 1.211 ± 0.03 | NA |
| navalC | 5.085 ± 0.01 | 5.408 ± 0.25 | 6.449 ± 0.17 | 5.904 ± 0.16 | 6.91 ± 0.05 | 7.192 ± 0.02 | 7.13 ± 0.01 |
| powerplant | -2.811 ± 0.01 | -58.377 ± 5.73 | -2.807 ± 0.01 | -2.792 ± 0.02 | -2.784 ± 0.01 | -2.782 ± 0.02 | NA |
| protein | -2.91 ± 0.01 | -14.811 ± 1.03 | -2.884 ± 0.01 | -2.849 ± 0.01 | -2.843 ± 0.00 | -2.842 ± 0.01 | -2.892 ± 0.00 |

Table 5.: RMSE and LPP for Experiment 2. †: Reported from Sun et al. (2019).

E. Implementation details

HMC. We consider the posterior distribution given by HMC (Betancourt, 2017) as a reference. In each case, the thinning was adjusted to retain a maximum of 10,000 samples. We used dual averaging to tune

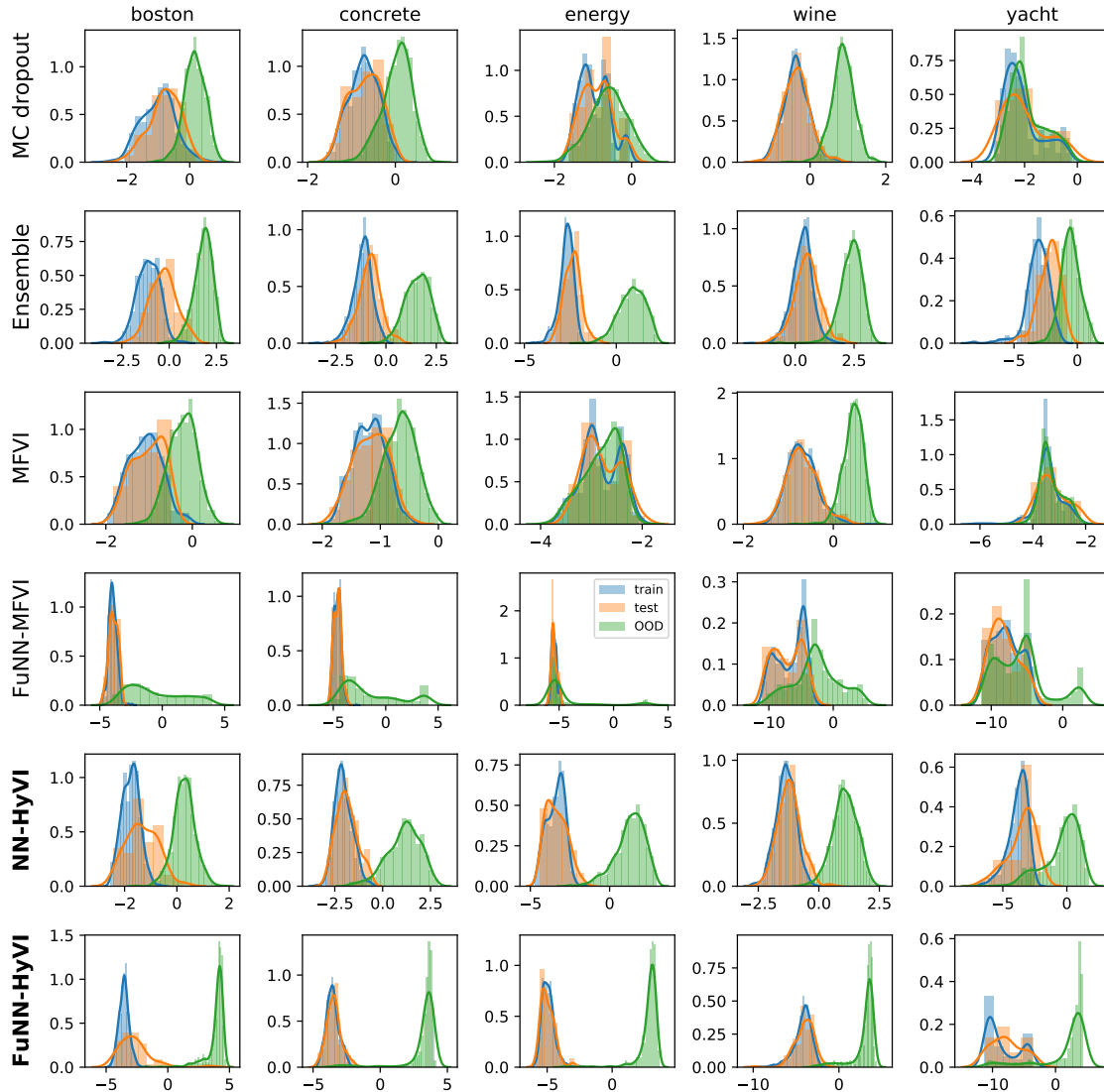


Figure 5.: Distributions of epistemic uncertainty on train, test and OOD input for various models on small UCI datasets (Exp. 2).

the step size and checked for convergence and efficiency using R -hat and effective sample size (ESS) for tails and bulk (Vehtari et al., 2019) .

We use the code of the `minimc` library (Carroll, 2019) with the parameters presented in Tab. 6.

MC dropout. We use a dropout probability of 0.05 and train the predictor network together with the likelihood noise σ_l with the log likelihood loss for $2K$ epochs using Adam optimizer with learning rate $lr=10^{-3}$ and weight decay equal to $10^{-\frac{1}{\sqrt{N}}}$ where N is the size of the data.

Ensemble. We independently train 5 models (10 for the synthetic dataset) for $3K$ epochs (500 for the large UCI datasets) with RMSE loss on mini-batches of size 50 (500 for the large UCI datasets) using stochastic gradient descent ($lr=0.01$, momentum=0.9).

| Dataset | number of iterations | burning | leapfrog steps |
|-------------------------------|----------------------|---------|----------------|
| Wave OOS Example | 120000 | 20000 | 200 |
| Wave Sparse Example | 120000 | 20000 | 200 |
| Wave Mixed Example | 230000 | 30000 | 250 |
| Boston Housing | 170000 | 40000 | 100 |
| Concrete Compressive Strength | 170000 | 40000 | 100 |
| Energy | 140000 | 4000 | 100 |
| Power Plant Combined Cycle | 60000 | 10000 | 100 |
| Wine Quality Red | 90000 | 20000 | 200 |
| Yacht Hydrodynamics | 140000 | 40000 | 100 |

Table 6.: Parameters used for the HMC.

MFVI. The parameters of the Gaussian posterior (jointly with the likelihood noise σ_l in Exp. 2) were trained using the ELBO as objective. The ELBO was approximated using 100 samples for the expected log likelihood and 500 samples for the MC estimate of the KL divergence. We used the same mini-batch size, optimizer and learning rate scheme as for NN-HyVI and FuNN-HyVI, except that we had to increase the patience by a factor of two in order to be able to fit the data.

F. Comparison of running time

Table 7 shows average running time in seconds for Experiment 2 on GPU (NVIDIA GeForce RTX 2080 Ti). We also included running times for HMC in Exp. 1 for the sake of comparison, but note that they were executed on Compute Canada’s CPUs and no real effort has been made to optimize the running time.

| | MC dropout | Ensemble | MFVI | FuNN-MFVI | HMC* | NN-HyVI | FuNN-HyVI |
|------------|------------|----------|------|-----------|------|---------|-----------|
| boston | 11 | 189 | 116 | 203 | 30K | 79 | 136 |
| concrete | 17 | 366 | 226 | 280 | 45K | 156 | 248 |
| energy | 13 | 273 | 191 | 217 | 30K | 96 | 242 |
| wine | 25 | 556 | 282 | 513 | 80K | 283 | 440 |
| yacht | 8 | 116 | 86 | 90 | 25K | 47 | 71 |
| kin8nm | 126 | 144 | 183 | 174 | NA | 93 | 135 |
| navalC | 187 | 212 | 574 | 296 | NA | 199 | 433 |
| powerplant | 149 | 177 | 153 | 164 | NA | 93 | 149 |
| protein | 777 | 825 | 912 | 1080 | NA | 504 | 890 |

Table 7.: Average running time on GPU in seconds for Exp. 2.

* : Obtained in Exp. 1 on CPU.